Climate Dynamics manuscript No.
(will be inserted by the editor)

Indications for a North Atlantic ocean circulation regime shift at the onset of the Little Ice Age

C.-F. Schleussner · D.V. Divine · J.F. Donges · A. Miettinen · R.V. Donner

Received: date / Accepted: date

Abstract A prominent characteristic of the reconstructed Northern Hemisphere temperature signal over the last millennium is the transition from the Medieval Climate Anomaly (MCA) to the Little Ice Age (LIA). Here we report indications for a non-linear regime shift in the North Atlantic ocean circulation during the onset of the Little Ice Age. Specifically, we apply a novel statistical test based on horizontal visibility graphs to two ocean sediment August sea-surface temperature records from the Norwegian Sea and the central subpolar basin and find robust indications of time-irreversibility in both records during the LIA onset. Despite a basin-wide cooling trend, we report an anomalous warming in the central subpolar basin during the LIA that is reproduced in ensemble simulations with the model of intermediate complexity CLIMBER-3α as a result of a non-linear regime shift in the subpolar North Atlantic ocean circulation. The identified volcanically triggered non-linear transition in the model simulations provides a plausible explanation for the signatures of time-irreversibility found in the ocean sediment records. Our findings indi-

C.F. Schleussner
Climate Analytics, Berlin, Germany
Potsdam Institute for Climate Impact Research, Potsdam, Germany
E-mail: schleussner@pik-potsdam.de

D. Divine
Norwegian Polar Institute, Fram Centre, Tromsø, Norway
Department of Mathematics and Statistics, University of Tromsø, Tromsø, Norway

J. F. Donges
Potsdam Institute for Climate Impact Research, Potsdam, Germany,
Stockholm Resilience Centre, Stockholm University, Stockholm, Sweden

A. Miettinen
Norwegian Polar Institute, Fram Centre, Tromsø, Norway

R. V. Donner
Potsdam Institute for Climate Impact Research, Potsdam, Germany

cate a potential multi-stability of the North Atlantic ocean circulation and its importance for regional climate change on centennial time scales.

Keywords Little Ice Age · Volcanic Forcing · Last Millennium · Horizontal Visibility Graphs · Time Series Irreversibility · Marine Sediments

1 Introduction

The transition from the Medieval Climate Anomaly (MCA) to the Little Ice Age (LIA) primarily in the Northern Hemisphere is one of the most important climatic shifts during the pre-industrial last millennium. Although recent paleoclimate reconstructions reveal no coherent global-scale cooling at the onset of the LIA, they agree on a generally colder period from the 16th to the 19th century (e.g. PAGES 2k (2013)). The IPCC's recent Fifth Assessment report defines the LIA as a period between 1450 and 1850 (Masson-Delmotte et al, 2013). In Europe, the regional expression of the LIA is associated with a spatially and temporally heterogeneous cooling, most pronounced in central and northern Europe (Büntgen et al, 2011; PAGES 2k, 2013). Modelling of these diverse changes remains challenging and recent intercomparisons of complex coupled model results over the last millennium exhibit considerable intermodel spread and deviations from reconstructions (Eby et al., 2013; Fernández-Donado et al, 2013).

Besides uncertainties in timing and extent, also the origin of this climate shift is still a subject of debate. Since the LIA coincides with several minima in the total solar irradiance (TSI), solar activity has been proposed as a possible driver already by Eddy (1976). The impact of TSI changes on the coupled ocean-atmosphere system in the North Atlantic has been investigated in a variety of different model studies since (e.g., Crowley, 2000; Zorita et al, 2004; Swingedouw et al, 2012). As an alternative hypothesis, volcanic eruptions have been suggested as the origin of the regional cooling (Robock, 1979; Crowley, 2000). Despite the short life-time of volcanic aerosol loadings, they have been found to influence North Atlantic climate variability on multi-decadal time scales (Otterå et al, 2010; Fischer et al, 2007; Zanchettin et al, 2011; Goosse et al, 2012). Decadally-paced volcanic eruptions have been reported to trigger coupled sea-ice oceanic feedbacks leading to a sustained slow-down of the Atlantic Meridional Overturning Circulation (AMOC) and persistent hemispheric cooling in modelling studies of the last millennium (Zhong et al, 2011; Miller et al, 2012; Schleussner and Feulner, 2013).

Here we test the hypothesis of a non-linear regime shift in the North Atlantic during the MCA-LIA transition based on an analysis of two fossil diatom-based high-resolution August sea surface temperature reconstructions from two ocean sediment cores from the central subpolar basin (Rapid 21-COM) and the Norwegian Sea (CR 948/2011) using a novel statistical test for time-irreversibility. We further compare our findings with ensemble simulations of the model of intermediate complexity CLIMBER-3α.

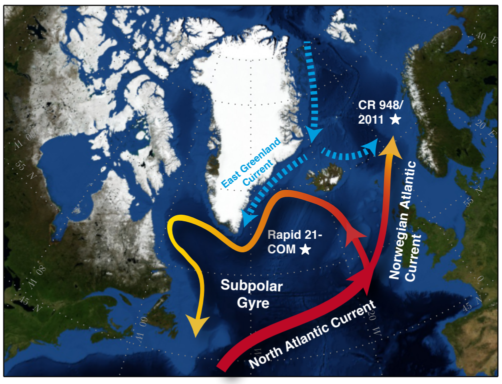

Fig. 1 Locations of the Rapid 21-COM and CR 948/2011 sediment cores and a schematic representation of major oceanic currents in the North Atlantic.

2 Materials and Methods

2.1 Marine sediment core data

Proxy-based reconstructions of August sea surface temperature (aSST) from two marine sediment cores from the northern North Atlantic are used in this study: Rapid 21-COM (Miettinen et al, 2012) recovered from the Reykjanes Ridge in the Iceland Basin (57°27.09′N, 27°54.53′W at 2630 m water depth (data available under NCDC/NOAA, 12905) and CR 948/2011 (Berner et al, 2011) from the Vøring Plateau in the Norwegian Sea (66°58.18′N, 07°38.36′E from 1020 m water depth (data available under NCDC/NOAA, 17475, see Fig. 1 for core locations).

Changes in the relative composition of diatomic assemblages in marine sediments during the considered period reflect the corresponding changes in oceanographic settings at the core sites. At the Vøring Plateau (CR 948/2011 site) the North Atlantic Current (NAC) and the Norwegian-Atlantic current assemblages (factors 2 and 4 as defined in Andersen et al, 2004)), typical for warmer and saline North Atlantic waters originating from the North Atlantic Drift, show a rapid decline being partly substituted by colder and fresher water dwelling diatoms of the east and west Greenland Current (factor 7) and sub-Arctic (factor 3) assemblages (Berner et al, 2011). At the Rapid 21-COM site the major surface changes are associated with a gradual decrease in the relative contribution of the dominant sub-Arctic (factor 3) assemblage with a parallel increase of the factor 2 assemblage linked with warm water masses of the North Atlantic Drift.

For both cores, a weighted averaging partial least-squares regression transfer function technique (WA-PLS, ter Braak and Juggins, 1993) was used to

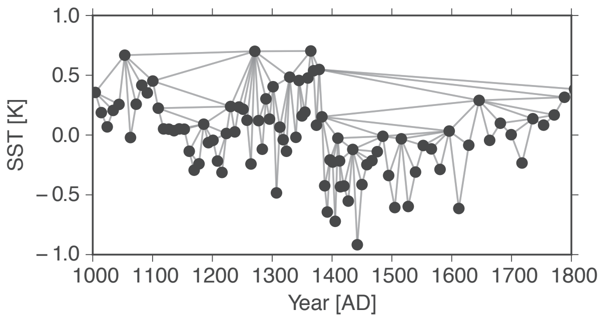

Fig. 2 Visualization of the horizontal visibility graph constructed for CR 948/2011. Each node represents a data point of the time series and edges between nodes are constructed following Eq. 1.

convert down-core diatom assemblages into past aSST estimates with an average resolution of about 8-10 years over the last millennium. Miettinen et al (2012) and Berner et al (2011) provide additional information on the individual records and the procedures used in the analysis of the Rapid 21-COM and the CR 948/2011 core data.

The data from the Rapid 21-COM (subpolar gyre) and the CR 948/2011 cores (Nordic seas) have been cropped to the time interval of interest between 1000 and 1800 AD. This leads to time series of 95 (Rapid 21-COM) and 91 (CR 948/2011) samples, respectively. The mean sampling interval of the Rapid 21-COM time series is 8.4 y with a standard deviation of 3.1 y. The mean sampling interval of the CR 948/2011 time series is 8.9 y with a standard deviation of 4.1 y. For both time series, the sampling interval is always smaller than approximately 20 years.

2.2 Testing for time series irreversibility

Beyond climatic trends and substantial variations on multi-centennial time scales present in both cores, higher-order properties of the time series that could potentially reveal signatures of nonlinear dynamical behaviour in the data are of great interest. Complex network based approaches (Newman, 2010) of time series analysis are a powerful tool for detecting nonlinear dynamical transitions and regime shifts (Donner et al, 2011), in particularly when studying palaeoclimate data (Donges et al, 2011a,b). Specifically, visibility graph analysis (Lacasa et al, 2008, 2009) has been applied in various geophysical fields (Donner and Donges, 2012), including the study of hurricane frequencies (Elsner et al, 2009), turbulence (Liu et al, 2010), wind speed measurements (Pierini et al, 2012), oceanic tidal records (Telesca et al, 2012), seismicity (Telesca and Lovallo, 2012; Aguilar-San Juan and Guzmán-Vargas, 2013; Telesca et al, 2013) and solar activity (Yu et al, 2012; Zou et al, 2014a,b).

Here, we apply a recently developed method by Donges et al (2013a) to test for time series irreversibility that is based on horizontal visibility graphs (HVGs, Luque et al, 2009; Lacasa et al, 2012; Telesca et al, 2014). HVGs are constructed from a time series $(x(t_i))_{i=1}^{N}$ such that each data point $x_i = x(t_i)$ of the time series is assigned to a node i of the graph. Two nodes i and j are connected by a link, if all scalar values x_k, $i < k < j$ are smaller than x_i and x_j. This results in the following expression for the graph's adjacency matrix A:

$$A_{ij} = \prod_{k=i+1}^{j-1} \Theta(x_i - x_k)\, \Theta(x_j - x_k), \tag{1}$$

where $\Theta(\cdot)$ denotes the Heaviside function. Figure 2 illustrates a visibility graph for CR 948/2011.

Our aim is to test the null hypothesis (NH) that the dynamics underlying the time series at hand is reversible. The rationale behind this is that consistent rejection of this NH points towards time-irreversibility, a hallmark of nonlinear dynamics (Theiler et al, 1992). In this paper, we adopt a statistical notion of time series reversibility: A stationary stochastic process or time series $\{x_i\}$ is called reversible if for arbitrary m, the tuples $(x_n, x_{n+1}, \ldots, x_{n+m})$ and $(x_{n+m}, x_{n+m-1}, \ldots, x_n)$ possess the same joint probability distribution (Lawrance, 1991). It is important to note that this definition of time series reversibility is distinct from more commonly known thermodynamic notions of the time reversibility of physical processes that derive from the second law of thermodynamics. Avoiding the curse of dimensionality in estimating high-dimensional joint probability distributions, statistical characteristics of the time-directed HVGs constructed from the time series can be tested (Lacasa et al, 2012; Donges et al, 2013a).

To this end, the time-directed network quantifiers degree

$$k_i^r = \textstyle\sum_{j<i} A_{ij}, \tag{2}$$

$$k_i^a = \textstyle\sum_{j>i} A_{ij} \tag{3}$$

and local clustering coefficient

$$\mathcal{C}_i^r = \binom{k_i^r}{2}^{-1} \textstyle\sum_{j<i,k<i} A_{ij} A_{jk} A_{ki}, \tag{4}$$

$$\mathcal{C}_i^a = \binom{k_i^a}{2}^{-1} \textstyle\sum_{j>i,k>i} A_{ij} A_{jk} A_{ki}. \tag{5}$$

are derived for each node i forward (advanced) and backward (retarded) in time. Subsequently, a Kolmogorov-Smirnov test is applied with the null hypothesis that the distribution of retarded and advanced degree (local clustering coefficient) are drawn from the same probability distribution, a necessary condition for reversible dynamics. In this sense, low p-values of this test indicate irreversible dynamics, while large p-values suggest reversible dynamics. All p-values given in the manuscript refer to the results of this Kolmogorov-Smirnov test for degree and local clustering coefficient, respectively. The NH of reversibility is rejected, if the p-value of the corresponding test statistics associated with a certain time series is smaller than a prescribed significance level (typically $p = 0.1$ or $p = 0.05$).

The test based on the local clustering coefficient (associated p-value p_C) is more sensitive than the degree-based test (associated p-value p_k) at the costs of a slightly larger false positive rate (Donges et al, 2013a). In the following, we apply both tests in parallel to ensure the robustness of our results. The approach can be employed with confidence to study short and irregularly sampled time series (Donner and Donges, 2012) such as the paleoclimate records that are of interest here (by construction, HVGs do not require a regular sampling on the time axis). We take advantage of the former property by applying the test in a sliding window mode to detect changes in the time reversibility structure and, thus, to identify potential nonlinear regime shifts in the data.

3 Results

3.1 Analysis of the ocean sediment records

Despite a basin-wide cooling in the whole North Atlantic, the Rapid 21-COM time series exhibits a warming during the LIA. On the contrary, CR 948/2011 shows an abrupt cooling after 1400, preceding the Rapid 21-COM warming by about 50 years (compare Fig. 3 left (right) panel for CR 948/2011 (Rapid 21-COM)). A cross-correlation function derived over the full time period of the two irregularly sampled time series using a Gaussian kernel method introduced by Rehfeld et al (2011) reveals a significant negative cross-correlation at a time lag of about 40 years (CR 948/2011 leads) that also prevails in a wavelet analysis (Miettinen et al, 2012). Our findings are in line with other high-resolution ocean sediment records, e.g. by Sicre et al (2014) who report a warming signal in the subpolar North Atlantic in contrast to a cooling in the Nordic Seas in sub-decadal ocean sediment records from North Iceland and North East Newfoundland. Signatures of a major environmental shift at the MCA-LIA transition are also reported from two calcite and quartz based sediment records from the Denmark Strait (Andrews and Jennings, 2014).

We performed a sliding window test for time series irreversibility as described above for both records over the pre-industrial last millennium from 1000 to 1800 AD (Fig. 3). Results for the degree and local clustering coefficient-based tests are depicted in the middle and bottom panel for different window sizes. The values of p_k and p_C are plotted at the time of the last sample contained in the corresponding window, thus taking only information from the past of this time step into account.

Since the concept of irreversibility refers to a time series, not to a specific point in time, a concrete timing of the irreversible dynamics is not trivial. The window size is varied between 30 and 60 data points, which comprises between 240 and 480 years given an average sampling time of approximately 8 years for both cores.

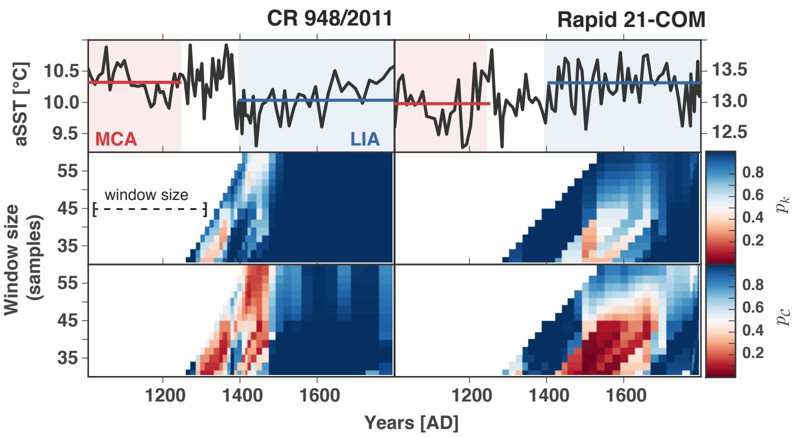

Fig. 3 Upper panels: Reconstructed aSST time series from the Nordic Seas (CR 948/2011, left) and the subpolar basin (Rapid 21-COM, right). The MCA (until 1250) and the LIA period (1400-1850) are shaded in red and blue, respectively, and the means over the MCA and LIA periods are depicted by the solid lines coloured accordingly. Central panels: Results of the degree-based HVG time series irreversibility tests (p_k) for different window sizes. p-values close to unity (blue) suggest reversibility, whereas such close to zero (red) point towards time-irreversibility. Bottom panels: Results of the local clustering coefficient-based tests (p_C).

We find a clear signature of time-irreversibility using the local clustering coefficient-based test with p-values $p_C < 0.05$ for Rapid 21-COM and window sizes below 45 data points between 1450 and 1600 and $p_C \leq 0.1$ for CR 948/2011 and all window sizes between 1300 and 1500 (see Fig. 3, bottom panels). This signal is robust over a wide range of consecutive windows during these periods but absent before and after in both cores, which indicates that the detected irreversibility originates from time series properties during the MCA-LIA transition.

The p-values for the degree-based test are somewhat higher (about 0.2, see Fig. 3, middle panel), which means that the NH cannot be rejected at a high significance level based on this test alone. Still, the timing of the signatures of NH rejection for the degree-based test matches very well with the local clustering coefficient-based test giving additional confidence in the results. It should be noted here that the results of visibility graph analysis have been shown to be robust with respect to irregular sampling and dating uncertainties of time series (Donner and Donges, 2012), further supporting the reliability of the our findings.

The PAGES 2k Consortium has identified several major volcanic-solar downturns over the last millennium (PAGES 2k, 2013) among which the first two down-turns between 1250 and 1300 and between 1400 and 1500 match well with the time-irreversibility signatures apparent in the two paleo time series. We relate the signal of time-irreversibility to the hypothesis of a coupled sea-ice ocean regime shift in the North Atlantic reported in several model simulations

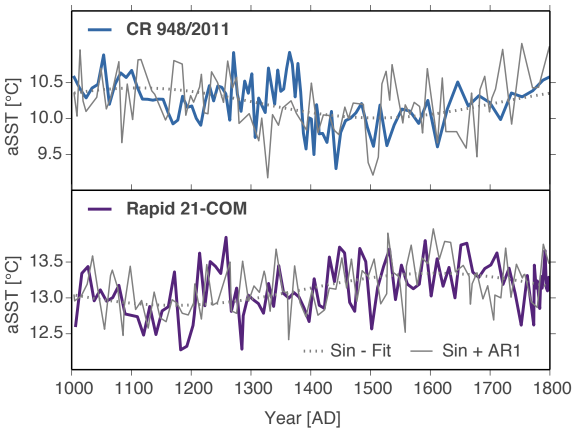

Fig. 4 Illustration of exemplary linear surrogates for the two ocean-sediment-core time series CR 948/2011 (upper panel) and Rapid 21-COM (lower panel). To account for multi-centennial variability, a sinusoidal (dashed grey) is fitted and stochastic variability is introduced by an AR1-process (light grey) matching the time series properties (see text for further details on the methodology).

of the last millennium (Zhong et al, 2011; Miller et al, 2012; Schleussner and Feulner, 2013) that are further discussed below. Remarkably, only the first two major volcanic-solar down-turns identified by the PAGES 2k Consortium leave a trace in our analysis, whereas later down-turns, e.g. after 1600 or around 1800, are not detected, which further supports the regime-shift hypothesis.

3.2 Statistical robustness

The complex network based time series irreversibility test introduced above is applied to the Rapid 21-COM and the CR 948/2011 core data by using sliding windows of different lengths. While shorter windows allow for higher temporal resolution, this also deteriorates the discriminatory power of the test, i.e., resulting in an increased rate of false positives (Donges et al, 2013a). Even though the test returns small p-values of 0.05 or 0.1 indicating a rejection of the null hypothesis of reversibility for the local clustering coefficient-based test for both cores (see Fig. 3), we cannot rule out that this is due to the detection of false positives.

To account for this possibility and further evaluate the robustness of our results, we apply a Monte Carlo test using linear surrogate time series of the individual records. Time series generated by linear processes are known to be reversible (Donges et al, 2013a) and, hence, rejections of the NH for such data represent false positives. An alternative hypothesis to a non-linear transition in the North Atlantic ocean circulation would be linear multi-centennial variability of the AMOC (Menary et al, 2011). We tested this hypothesis by fitting

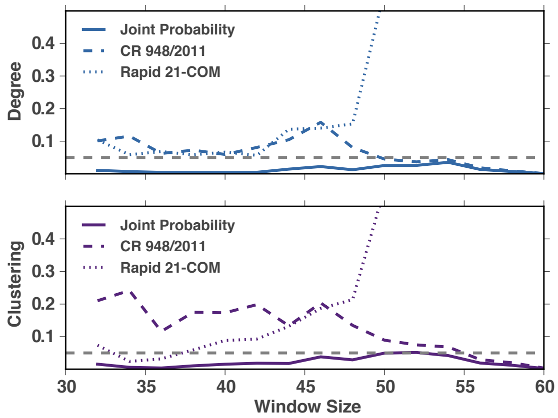

Fig. 5 Probability of the occurrence of p-values less or equal to the minimum for the CR 948/2011 (dashed, over the period 1300-1500) and Rapid 21-COM (dotted, over the period 1400-1600) in an N=10,000 ensemble of fully-linear surrogates of the two time series. The straight line gives the joint probability as the product of both. The grey dashed line denotes the $p = 0.05$ level.

a sinusoidal to both time series with periods of about 800 years for the CR 948/2011 and about 900 years for the Rapid 21-COM. The parameters of a first-order autoregressive process (AR1) are estimated using a Gaussian kernel function (Rehfeld et al, 2011) for the residual time series (record minus sinusoidal fit), which returns values for the autoregressive coefficient ϕ of 0.4 (0.01) for the CR 948/2011 (Rapid 21-COM) and a noise term with variance 0.1 K^2 for both time series. The realizations of the AR1 process are then added to the fitted sinusoidal. Finally, to account for the irregular sampling of the original records, the surrogates are subsampled. For this subsampling, the sampling time distribution of the original cores is preserved but shuffled in time. Figure 4 illustrates surrogate time series based on a linear sinusoidal plus an AR1 process in comparison with the original time series.

The analysis of the two ocean sediment core records reveals not only signatures of irreversibility in both time series, but also that the timing of these signatures between 1300 and 1500 for CR 948/2011 and between 1400 and 1600 for Rapid 21-COM matches well with the hypothesis of an underlying non-linearity at the MCA-LIA transition. We use an ensemble of N=10,000 surrogate time series that are constructed as described above to test the null hypothesis that false positives occur in both cores specifically during the 1300 – 1500 period (CR 948/2011) and the 1400 – 1600 period (Rapid 21-COM).

We derive the window-size dependent minimal p-value from both original time series over the relevant time intervals and estimate the probability of lower or equal p-values as a result of false positives from linear surrogates. The results of this test are depicted in Fig. 5. Even though false positives in the individual cores might occur with a probability of 0.05 and above (depending

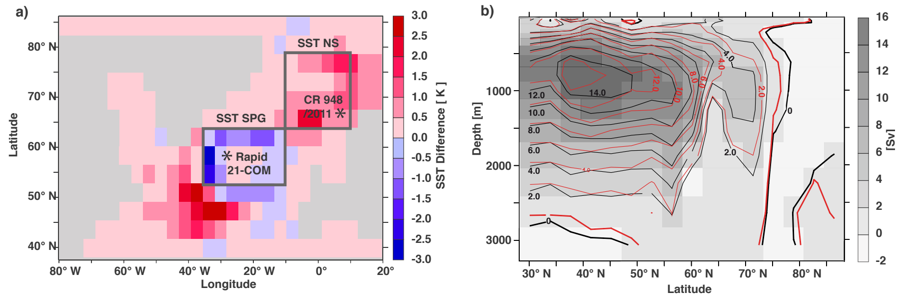

Fig. 6 Differences in sea-surface temperature (a) and zonally integrated meridional overturning stream-function (b) between the MCA (1050-1250 AD) and the LIA (1400-1800 AD) in the CLIMBER-3α ensemble mean. The locations of the Rapid 21-COM and CR 948/2011 sediment cores as well as the model SST boxes are highlighted in (a), whereas (b) depicts the MCA stream-function (grey background shading and black contour lines) and the LIA stream-function (red contour lines).

on the window size) for the individual cores (dashed and dotted lines), the joint probability of two false positives occurring in both time series as the product of both is below 0.05 for all window sizes and below 0.01 for small window sizes between 32 and 40 for the degree-based test. This estimate is based on the assumption that the occurrence of false positives is statistically independent in both ocean sediment records. Given the different core locations, sampling times as well as fundamentally different dynamics over the time period investigated, this assumption is justified. In summary, this test for robustness of the results reported in Section 3.1 indicates that millennial-scale trends with superposed autocorrelated noise are unlikely to give rise to false signatures of time-irreversibility during intervals that are consistent with the MCA-LIA transition at both core locations.

3.3 Comparison with ensemble simulations of the last millennium with CLIMBER-3α

In Schleussner and Feulner (2013), a volcanically triggered regime shift in the North Atlantic as the result of coupled sea-ice - ocean feedbacks is reported during the MCA-LIA transition in ensemble simulations of the model of intermediate complexity CLIMBER-3α forced by stochastically reconstructed wind-stress fields (more details on the model as well as on the simulations of the last millennium can be found in the Appendix). The modelled SST differences in the North Atlantic between the MCA and LIA shown in Fig. 6 match well with the observed opposed cooling and warming in the Nordic Seas and the subpolar basin apparent in the ocean sediment cores (see Fig. 3 upper panel).

The non-linear regime shift identified in Schleussner and Feulner (2013) is triggered by decadally-paced volcanic eruptions that lead to an increase of Nordic Sea sea-ice extent hindering deep-convection in the Nordic seas. This in turn prompts a reduction of the overflows over the Greenland-Scotland ridge (compare Fig. 6 (b)) and leads to increased re-circulation of subtropical waters in the subpolar basin strengthening convection in the central subpolar basin due to a positive surface salinity feedback. The strengthening of convection results in a densification of the gyre center and eventually leads to a baroclinic spin-up of the circulation that entrains more North Atlantic current waters closing the feedback loop (Levermann and Born, 2007; Mengel et al, 2012). At the same time, this circulation regime shift results in an AMOC slow-down (compare Fig. 7 (c)) leading to a basin-wide cooling that is consistent with multi-proxy reconstructions by Mann et al (2009) (Fig. 7(f)).

SST time series from the ensemble of CLIMBER-3α simulations for the central subpolar gyre (SPG) and the Nordic Seas are shown in Fig. 7(d) and (e). As in the sediment records we find an abrupt cooling in the Nordic Seas that precedes a more gradual subpolar warming in the model simulations and report signatures of time-irreversibility in the SST time series of the individual ensemble members pointing towards an underlying non-linear transition (see Appendix). However, great caution has to be taken when interpreting the actual timing of the transition in the individual ensemble runs due to the stochastic nature of the wind-stress forcing applied and apparent limitations of coarse resolution models like CLIMBER-3α in reproducing North Atlantic ocean dynamics on decadal time scales.

4 Discussion and Conclusion

By combining reconstructions, modern time series analysis methods and model simulations we find multiple indications for the existence of a marked non-linearity in the North Atlantic regional climate system that might have contributed to the onset of the LIA during the last millennium. Our statistical tests indicate time-irreversibility in two aSST time series reconstructed from ocean sediment cores from the Nordic Seas and the central subpolar basin at the MCA-LIA transition. Besides the time-irreversibility, both records exhibit opposing changes in SST during the MCA-LIA transition - while we observe an abrupt cooling in the Nordic Seas, the subpolar basin time series shows a delayed and more gradual warming trend in contrast to a basin-wide cooling during the LIA. We find these characteristics to be reproduced in ensemble simulations with the model of intermediate complexity CLIMBER-3α as a result of a volcanically triggered regime shift in the subpolar gyre circulation (Schleussner and Feulner, 2013). Regional non-linear transitions in the North Atlantic have also been reported in different complex coupled models (Semenov et al, 2009; Schulz et al, 2007; Jungclaus et al, 2014) as well as paleo-records (Moffa-Sánchez et al, 2014; Gennaretti et al, 2014). Model simulations by Zhong et al (2011) as well as Miller et al (2012) suggest a circulation regime shift due to volcanically triggered coupled sea-ice ocean feedbacks as the origin of the MCA-LIA transition. Such a non-linearity in the behaviour of the climate system may also have implications for regional proxy-based recon-

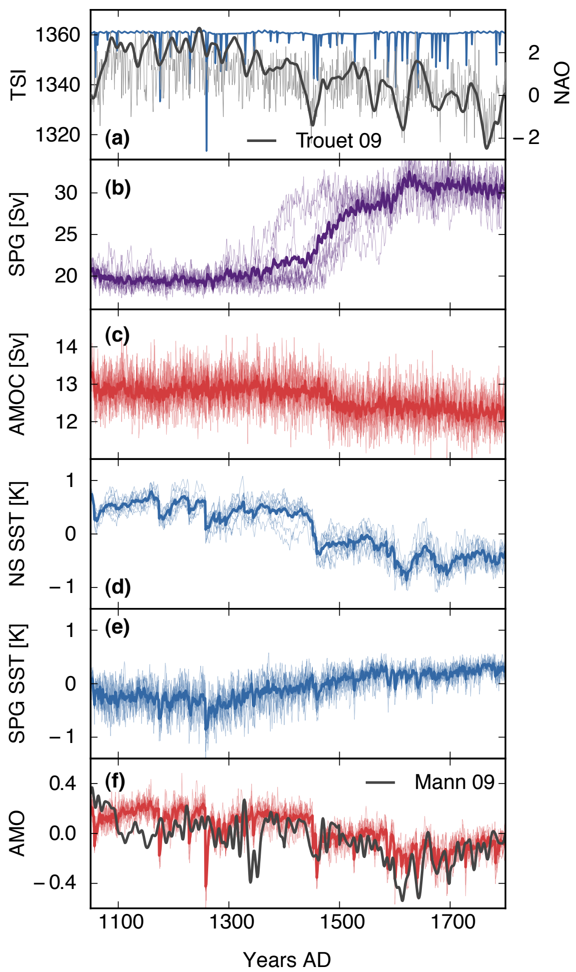

Fig. 7 The last millennium experiment is forced with prescribed TSI based on reconstructions from Steinhilber et al (2009) and volcanic forcing from Crowley (2000) (panel (a), blue line). As described in Schleussner and Feulner (2013) we perform ensemble simulations using 10 stochastically generated wind-stress forcings based on a NAO reconstruction by Trouet et al (2009). NAO reconstruction (dark grey line) as well as an illustrative stochastically generated time series (light grey line) are shown in panel (a) (right axis). Transient SPG (b) and AMOC (c) dynamics are depicted for the individual ensemble runs (light) as well as the ensemble mean (bold). SST anomalies for the SPG (65°-80° N and 10° W–10° E) and Nordic Sea region (50°-65° N and 37° –10° W, see boxes in Fig. 6) are shown in (d) and (e). Panel (f) depicts the AMO index anomalies in comparison with the multi-proxy reconstructions by Mann et al (2009).

structions of past climate and underlines the importance of short-lived, but strong perturbations (as e.g induced by volcanic eruptions) for the dynamics of the North Atlantic ocean (Otterå et al, 2010; Goosse et al, 2012). While more research on the North Atlantic climatic system is needed to further validate our findings, our results may have implications for the assessment of present-day ocean circulation stability in the North Atlantic in particular in the light of the dramatic reduction in Northern Hemisphere sea-ice over the last decades (Kinnard et al, 2011; Stroeve et al, 2011).

Acknowledgements The authors wish to thank Georg Feulner for helpful comments and suggestions and two anonymous reviewers for their comments that helped to improve the manuscript. This work was supported by the Deutsche Bundesstiftung Umwelt, the Stordalen Foundation, the Potsdam Institute for Climate Impact Research (PIK), and the German Federal Ministry for Science and Education (Project CoSy-CC^2, Grant No. 01LN1306A, and project GLUES). Visibility graph analysis was performed using the Python package `pyunicorn` developed at PIK (Donges et al, 2013b) that is available at `http://tocsy.pik-potsdam.de/pyunicorn.php`.

Appendix

A Ensemble simulations of the last millennium with CLIMBER-3α

In this appendix, we present further details on the ensemble simulations of the last millennium with CLIMBER-3α as well as results of the time-irreversibility test applied to the model output.

A.1 Model description

CLIMBER-3α is a model of intermediate complexity (Montoya et al, 2005). It's oceanic component is based on the GFDL MOM-3 code (Pacanowski and Griffies, 1999), with 24 variably spaced vertical levels, a coarse horizontal resolution of 3.75°, a background vertical diffusivity of $\kappa_h = 0.3 \times 10^{-4}\,\mathrm{m}^2\,\mathrm{s}^{-1}$ and an eddy-induced tracer advection with a thickness diffusion coefficient of $\kappa_{gm} = 250\,\mathrm{m}^2\,\mathrm{s}^{-1}$. It contains a coarse resolution statistical-dynamical atmosphere (Petoukhov et al, 2000) and a thermodynamic/dynamic sea-ice component (Fichefet and Maqueda, 1997).

Although this model's coarse resolution and the simplified atmosphere clearly limit its prognostic capabilities at regional scales, CLIMBER-3α has been found to reproduce large-scale characteristics of the global climate system and has been used in a variety of model intercomparison studies for the last millennium and future projections of the stability of the AMOC (Jansen et al, 2007; Eby et al., 2013; Gregory et al, 2005; Stouffer et al, 2006).

A.2 Ensemble simulations of the last millennium

In the simulations over the last millennium presented here, we applied TSI reconstructions by Steinhilber et al (2009) and volcanic forcing by Crowley (2000) as well as anthropogenic aerosols and greenhouse gas forcing following the PMIP3 recommendations (Schmidt et al, 2011). The combined TSI is shown in Fig. 7(a).

Based on a reconstruction of the North Atlantic Oscillation (NAO) by Trouet et al (2009) as the leading mode of atmospheric variability in the North Atlantic, we stochastically generated an ensemble of 10 independent representations of wind-stress fields for the last millennium (similar to an approach by Sedláček and Mysak (2009), see Schleussner and Feulner (2013) for further details on the method). For illustration purposes, the NAO record by Trouet et al (2009) as well as one example reconstruction are depicted in Fig. 7(a).

It is important to highlight that the response of the North-Atlantic ocean in the ensemble simulations on multi-decadal to centennial time scales is dominated by the coupled sea-ice - ocean mechanism identified (Schleussner and Feulner, 2013), although the NAO reconstruction by Trouet et al (2011) indicates a shift from a persistent positive NAO to a more oscillatory regime during the MCA-LIA transition. While this persistent positive NAO phase during the MCA is not reproduced by complex coupled climate models (Lehner et al, 2012), a less prominent shift in the atmospheric conditions between MCA and LIA would not affect the main findings presented here.

A.3 Bistability in the subpolar gyre circulation in CLIMBER-3α

CLIMBER-3α exhibits a regime shift in the subpolar gyre circulation with respect to the convection strength in its centre (Levermann and Born, 2007) that can be triggered by a variety of forcings, e.g. applying a very weak freshwater offset of the order of 15 mSv over the Nordic Sea convection side. Mengel et al (2012) found that the oceanic response to atmospheric variability in CLIMBER-3α performs best in reproducing observed levels close to the threshold of the circulation regime. While this multi-stability can also be a result of the coarse resolution and other shortcomings of the specific model, signatures of multi-stability have also been found in a variety of complex coupled models (Born et al, 2013; Schulz et al, 2007).

While the regime shift itself is a robust finding also without additional freshwater budget adjustment (Schleussner and Feulner, 2013), the best match with reconstructed data is achieved for a constant freshwater offset of 5 mSv over the convective region in the Nordic Seas (63.75°-78.75° N and 11.25° W–10° E). This adjustment is within the range of observed natural variability since the 1950s (Curry and Mauritzen, 2005). The actual timing of this transition shows a considerable ensemble spread, thus indicating the importance of atmospheric conditions, and is also very sensitive to minor changes in the freshwater budget. It is important to highlight the conceptual nature of the results presented here, since models of intermediate complexity like CLIMBER-3α are not suitable to provide realistic transient dynamics on short time scales, but rather indicate possible mechanisms for transition.

B Time series irreversibility analysis for the CLIMBER-3α simulations

Simulations with CLIMBER-3α reveal a non-linear regime shift in the subpolar North Atlantic at the MCA-LIA transition that should be detectable using the time series irreversibility analysis technique applied here. Fig. A1 summarizes the results of the time series irreversibility analysis for the annual Nordic Seas and subpolar basin area-averaged SST signals. It depicts for each time step the median (the p-values for 5 out of 10 ensemble members are equal or below this value at this time step) and the 30 % quantile (the p-values for 3 out of 10 ensemble members are equal or below this value at this time step). Due to the prescribed atmospheric forcing applied, potential signatures of time-irreversibility in the SST signal in the CLIMBER-3α ensemble simulations may not evolve as they would without it and we can only speculate about the actual effect of this prescription on the highly sensitive analysis methods. This represents a serious limitation and neither the results for individual ensemble members nor the quantile estimates should be directly compared to the results for the individual paleo-record time series presented in Fig. 3. We show the quantile values to give an indication, where the time series reversibility test leads to rejection of the NH in the CLIMBER-3α ensemble simulations bearing the limitations discussed above in mind.

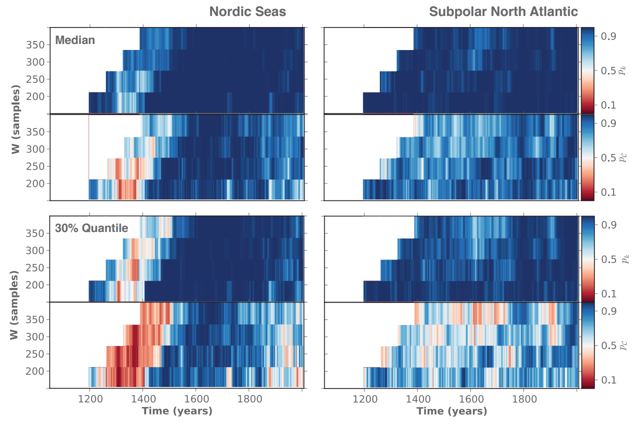

Fig. A1 Time series reversibility test for the CLIMBER-3α ensemble simulations with an annual sampling time. Left (right) panel: SST record averaged over the Nordic Seas (subpolar basin). See Fig. 1 for the region and Fig. 7 for the corresponding time series. The upper panels denote median p-values (p_k: degree-based test, p_c: local clustering coefficient-based test) over the model ensemble and the lower panels give the 30 % quantile.

References

Aguilar-San Juan B, Guzmán-Vargas L (2013) Earthquake magnitude time series: scaling behavior of visibility networks. European Physical Journal B 86(11)

Andersen C, Koç N, Jennings A, Andrews JT (2004) Nonuniform response of the major surface currents in the Nordic Seas to insolation forcing: Implications for the Holocene climate variability. Paleoceanography 19:PA2003, DOI 10.1029/2002PA000873

Andrews JT, Jennings AE (2014) Multidecadal to millennial marine climate oscillations across the Denmark Strait (66° N) over the last 2000 cal yr BP. Climate of the Past 10(1):325–343, DOI 10.5194/cp-10-325-2014

Berner KS, Ko N, Godtliebsen F, Divine D (2011) Holocene climate variability of the norwegian atlantic current during high and low solar insolation forcing. Paleoceanography 26(2):PA2220, DOI 10.1029/2010PA002002

Born A, Stocker TF, Raible CC, Levermann A (2013) Is the Atlantic subpolar gyre bistable in comprehensive coupled climate models? Climate Dynamics 40(11-12):2993–3007, DOI 10.1007/s00382-012-1525-7

ter Braak CJ, Juggins S (1993) Weighted averaging partial least squares regression (wa-pls): an improved method for reconstructing environmental variables from species assemblages. Hydrobiologia 269-270(1):485–502, DOI 10.1007/BF00028046

Büntgen U, Tegel W, Nicolussi K, McCormick M, Frank D, Trouet V, Kaplan JO, Herzig F, Heussner KU, Wanner H (2011) 2500 Years of European Climate Variability and Human Susceptibility. Science 331:578–582, DOI 10.1126/science.1197175

Crowley T (2000) Causes of climate change over the past 1000 years. Science 289(5477):270–277, DOI 10.1126/science.289.5477.270

Curry R, Mauritzen C (2005) Dilution of the northern North Atlantic Ocean in recent decades. Science 308(5729):1772–1774, DOI 10.1126/science.1109477

Donges JF, Donner RV, Rehfeld K, Marwan N, Trauth MH, Kurths J (2011a) Identification of dynamical transitions in marine palaeoclimate records by recurrence network analysis. Nonlinear Processes in Geophysics 18(5):545–562, DOI 10.5194/npg-18-545-2011

Donges JF, Donner RV, Trauth MH, Marwan N, Schellnhuber HJ, Kurths J (2011b) Nonlinear detection of paleoclimate-variability transitions possibly related to human evolution. Proceedings of the National Academy of Science of the USA 108(51):20,422–20,427, DOI

10.1073/pnas.1117052108
Donges JF, Donner RV, Kurths J (2013a) Testing time series irreversibility using complex network methods. Europhysics Letters 102(1):10,004, DOI 10.1209/0295-5075/102/10004
Donges JF, Heitzig J, Runge J, Schultz HC, Wiedermann M, Zech A, Feldhoff J, Rheinwalt A, Kutza H, Radebach A, et al (2013b) Advanced functional network analysis in the geosciences: The pyunicorn package. Geophysical Research Abstracts 15:3558
Donner RV, Donges JF (2012) Visibility graph analysis of geophysical time series: Potentials and possible pitfalls. Acta Geophysica 60(3):589–623, DOI 10.2478/s11600-012-0032-x
Donner R, Small M, Donges J, Marwan N, Zou Y, Xiang R, Kurths J (2011) Recurrence-based time series analysis by means of complex network methods. International Journal of Bifurcation and Chaos 21(4):1019–1046, DOI 10.1142/S0218127411029021
Eby, M., Weaver, A. J., Alexander, K., Zickfeld, K., Abe-Ouchi, A., Cimatoribus, A. A., Crespin, E., Drijfhout, S. S., Edwards, N. R., Eliseev, A. V., Feulner, G., Fichefet, T., Forest, C. E., Goosse, H., Holden, P. B., Joos, F., Kawamiya, M., Kicklighter, D., Kienert, H., Matsumoto, K., Mokhov, I. I., Monier, E., Olsen, S. M., Pedersen, J. O. P., Perrette, M., Philippon-Berthier, G., Ridgwell, A., Schlosser, A., Schneider von Deimling, T., Shaffer, G., Smith, R. S., Spahni, R., Sokolov, A. P., Steinacher, M., Tachiiri, K., Tokos, K., Yoshimori, M., Zeng, N., and Zhao, F.: Historical and idealized climate model experiments: an intercomparison of Earth system models of intermediate complexity, Climate of the Past, 9, 1111-1140, DOI 10.5194/cp-9-1111-2013, 2013.
Eddy J (1976) The maunder minimum. Science 192(4245):1189–1202
Elsner J, Jagger T, Fogarty E (2009) Visibility network of united states hurricanes. Geophysical Research Letters 36(16)
Fernández-Donado L, González-Rouco JF, Raible CC, Ammann CM, Barriopedro D, García-Bustamante E, Jungclaus JH, Lorenz SJ, Luterbacher J, Phipps SJ, Servonnat J, Swingedouw D, Tett SFB, Wagner S, Yiou P, Zorita E (2013) Temperature response to external forcing in simulations and reconstructions of the last millennium. Climate of the Past 9:393–421, DOI 10.1038/ngeo955
Fichefet T, Maqueda MAM (1997) Sensitivity of a global sea ice model to the treatment of ice thermodynamics and dynamics. Journal of Geophysical Research 102:12,609–12,646
Fischer EM, Luterbacher J, Zorita E, Tett SFB, Casty C, Wanner H (2007) European climate response to tropical volcanic eruptions over the last half millennium. Geophysical Research Letters 34(5):L05,707, DOI 10.1029/2006GL027992
Gennaretti F, Arseneault D, Nicault A, Perreault L, Bégin Y (2014) Volcano-induced regime shifts in millennial tree-ring chronologies from northeastern North America. Proceedings of the National Academy of Sciences of the USA (22), DOI 10.1073/pnas.1324220111
Goosse H, Crespin E, Dubinkina S, Loutre MF, Mann ME, Renssen H, Sallaz-Damaz Y, Shindell D (2012) The role of forcing and internal dynamics in explaining the Medieval Climate Anomaly. Climate Dynamics 39(12):2847–2866, DOI 10.1007/s00382-012-1297-0
Gregory JM, Dixon KW, Stouffer RJ, Weaver AJ, Driesschaert E, Eby M, Fichefet T, Hasumi H, Hu A, Jungclaus JH, Kamenkovich IV, Levermann A, Montoya M, Murakami S, Nawrath S, Oka A, Sokolov AP, Thorpe RB (2005) A model intercomparison of changes in the Atlantic thermohaline circulation in response to increasing atmospheric CO_2 concentration. Geophysical Research Letters 32:L12,703, DOI 10.1029/2005GL023209
Jansen E, Overpeck J, Briffa K, Duplessy JC, Joos F, Masson-Delmotte V, Olago D, Otto-Bliesner B, Peltier WR, Rahmstorf S, Ramesh R, Raynaud D, Rind D, Solomina O, Villalba R, Zhang D (2007) Climate Change 2007: The Physical Science Basis. Contribution of Working Group I to the Fourth Assessment Report of the Intergovernmental Panel on Climate Change. Cambridge University Press, Cambridge, United Kingdom and New York, NY, USA.
Jungclaus JH, Lohmann K, Zanchettin D (2014) Enhanced 20th century heat transfer to the Arctic simulated in the context of climate variations over the last millennium. Climate of the Past, 10, 2201-2213, 2014, DOI 10.5194/cp-10-2201-2014
Kinnard C, Zdanowicz CM, Fisher DA, Isaksson E, de Vernal A, Thompson LG (2011) Reconstructed changes in Arctic sea ice over the past 1,450 years. Nature 479(7374):509–512, DOI 10.1038/nature10581
Lacasa L, Luque B, Ballesteros F, Luque J, Nuno J (2008) From time series to complex networks: The visibility graph. Proceedings of the National Academy of Sciences of the

United States of America 105(13):4972–4975, DOI 10.1073/pnas.0709247105
Lacasa L, Luque B, Luque J, Nuno J (2009) The visibility graph: A new method for estimating the Hurst exponent of fractional Brownian motion. Europhysics Letters 86(3):30,001, DOI 10.1209/0295-5075/86/30001
Lacasa L, Nuñez A, Roldán É, Parrondo JM, Luque B (2012b) Time series irreversibility: a visibility graph approach. European Physical Journal B 85:217, DOI 10.1140/epjb/e2012-20809
Lawrance AJ (1991) Directionality and reversibility in time-series. Int Stat Rev 59(1):67–79, DOI 10.2307/1403575
Lehner F, Raible CC, Stocker TF (2012) Testing the robustness of a precipitation proxy-based North Atlantic Oscillation reconstruction. Quaternary Science Reviews 45:85–94, DOI 10.1016/j.quascirev.2012.04.025
Levermann A, Born A (2007) Bistability of the subpolar gyre in a coarse resolution climate model. Geophysical Research Letters 34:L24,605, DOI 10.1029/2007GL031732
Liu C, Zhou WX, Yuan WK (2010) Statistical properties of visibility graph of energy dissipation rates in three-dimensional fully developed turbulence. Physica A, 389(13):2675–2681
Luque B, Lacasa L, Ballesteros F, Luque J (2009) Horizontal visibility graphs: Exact results for random time series. Physical Review E 80(4):046,103
Mann ME, Zhang Z, Rutherford S, Bradley RS, Hughes MK, Shindell D, Ammann C, Faluvegi G, Ni F (2009) Global signatures and dynamical origins of the Little Ice Age and Medieval Climate Anomaly. Science 326(5957):1256–60, DOI 10.1126/science.1177303
Masson-Delmotte V, Schulz M, Abe-Ouchi A, Beer J, Ganopolski A, González Rouco J, Jansen E, Lambeck K, Luterbacher J, Naish T, Osborn T, Otto-Bliesner B, Quinn T, Ramesh R, Rojas M, Shao X, Timmermann A (2013) Information from Paleoclimate Archives. In: Stocker, TF, D Qin, G-K Plattner, M Tignor, SK Allen, J Boschung, A Nauels, Y Xia VB, (eds) PM (eds) Climate Change 2013: The Physical Science Basis. Contribution of Working Group I to the Fifth Assessment Report of the Intergovernmental Panel on Climate Change, Cambridge University Press, Cambridge, United Kingdom and New York, NY, USA
Menary MB, Park W, Lohmann K, Vellinga M, Palmer MD, Latif M, Jungclaus JH (2011) A multimodel comparison of centennial Atlantic meridional overturning circulation variability. Climate Dynamics 38(11-12):2377–2388, DOI 10.1007/s00382-011-1172-4
Mengel M, Levermann A, Schleussner CF, Born A (2012) Enhanced Atlantic subpolar gyre variability through baroclinic threshold in a coarse resolution model. Earth System Dynamics 3(2):189–197, DOI 10.5194/esd-3-189-2012
Miettinen A, Divine D, Koç N, Godtliebsen F, Hall IR (2012) Multicentennial Variability of the Sea Surface Temperature Gradient across the Subpolar North Atlantic over the Last 2.8 kyr. Journal of Climate 25:4205–4219, DOI 10.1175/JCLI-D-11-00581.1
Miller GH, Geirsdóttir A, Zhong Y, Larsen DJ, Otto BL, Holland MM, Bailey DA, Refsnider KA, Lehman SJ, John R (2012) Abrupt onset of the Little Ice Age triggered by volcanism and sustained by sea-ice / ocean feedbacks. Geophysical Research Letters 39:L02,708, DOI 10.1029/2011GL050168
Moffa-Sánchez P, Hall IR, Barker S, Thornalley DJR, Yashayaev I (2014) Surface changes in the eastern Labrador Sea around the onset of the Little Ice Age. Paleoceanography 28:160–175, DOI 10.1002/2013PA002523
Montoya M, Griesel A, Levermann A, Mignot J, Hofmann M, Ganopolski A, Rahmstorf S (2005) The Earth System Model of Intermediate Complexity CLIMBER-3α. Part I: description and performance for present day conditions. Climate Dynamics 25:237–263, DOI 10.1007/s00382-005-0044-1
NCDC/NOAA data base ID Cr 948/2011: 17475. www.ncdc.noaa.gov
NCDC/NOAA data base ID Rapid 21-COM: 12905. www.ncdc.noaa.gov
Newman MEJ (2010) Networks: An Introduction. Oxford University Press, Oxford
Otterå O, Bentsen M, Drange H, Suo L (2010) External forcing as a metronome for Atlantic multidecadal variability. Nature Geoscience 3(10):688–694, DOI 10.1038/ngeo955
Pacanowski RC, Griffies SM (1999) The MOM-3 manual. Tech. Rep. 4, NOAA/Geophyical Fluid Dynamics Laboratory, Princeton, NJ, USA

PAGES 2k Consortium (2013) Continental-scale temperature variability during the past two millennia. Nature Geoscience 6:339–346, DOI 10.1038/ngeo1797

Petoukhov V, Ganopolski A, Brovkin V, Claussen M, Eliseev A, Kubatzki C, Rahmstorf S (2000) CLIMBER-2: a climate system model of intermediate complexity. Part I: model description and performance for present climate. Climate Dynamics 16:1–17, DOI 10.1007/PL00007919

Pierini JO, Lovallo M, Telesca L (2012) Visibility graph analysis of wind speed records measured in central argentina. Physica A 391(20):5041–5048

Rehfeld K, Marwan N, Heitzig J, Kurths J (2011) Comparison of correlation analysis techniques for irregularly sampled time series. Nonlinear Processes in Geophysics 18(3):389–404, DOI 10.5194/npg-18-389-2011

Robock A (1979) The "Little Ice Age": Northern Hemisphere Average Observations and Model Calculations. Science 206(4425):1402–1404

Schleussner CF, Feulner G (2013) A volcanically triggered regime shift in the subpolar North Atlantic Ocean as a possible origin of the Little Ice Age. Climate of the Past 9(3):1321–1330, DOI 10.5194/cp-9-1321-2013

Schmidt G, Jungclaus J, Ammann C, Bard E, Braconnot P, Crowley T, Delaygue G, Joos F, Krivova N, Muscheler R, et al (2011) Climate forcing reconstructions for use in PMIP simulations of the last millennium (v1. 0). Geoscientific Model Development 4:33–45, DOI 10.5194/gmd-4-33-2011

Schulz M, Prange M, Klocker A (2007) Low-frequency oscillations of the Atlantic Ocean meridional overturning circulation in a coupled climate model. Climate of the Past 3(1):97–107

Sedláček, J. and Mysak, L. A.: Sensitivity of sea ice to wind-stress and radiative forcing since 1500: a model study of the Little Ice Age and beyond, Climate Dynamics, 32, 817–831, DOI 10.1007/s00382-008-0406-6, 2009.

Semenov V, Park W, Latif M (2009) Barents Sea inflow shutdown: A new mechanism for rapid climate changes. Geophysical Research Letters 36 (L14709), DOI 200910.1029/2009GL038911

Sicre MA, Weckström K, Seidenkrantz MS, Kuijpers A, Benetti M, Masse G, Ezat U, Schmidt S, Bouloubassi I, Olsen J, Khodri M, Mignot J (2014) Labrador current variability over the last 2000 years. Earth and Planetary Science Letters 400:26–32, DOI 10.1016/j.epsl.2014.05.016

Steinhilber F, Beer J, Fröhlich C (2009) Total solar irradiance during the Holocene. Geophysical Research Letters 36:L19,704, DOI 10.1029/2009GL040142

Stouffer RJ, Yin J, Gregory JM, Dixon KW, Spelman MJ, Hurlin W, Weaver AJ, Eby M, Flato GM, Hasumi H, Hu A, Jungclaus JH, Kamenkovich IV, Levermann A, Montoya M, Murakami S, Nawrath S, Oka A, Peltier WR, Robitaille DY, Sokolov AP, Vettoretti G, Weber SL (2006) Investigating the Causes of the Response of the Thermohaline Circulation to Past and Future Climate Changes. Journal of Climate 19(8):1365–1387, DOI 10.1175/JCLI3689.1

Stroeve JC, Serreze MC, Holland MM, Kay JE, Malanik J, Barrett AP (2011) The Arctic's rapidly shrinking sea ice cover: a research synthesis. Climatic Change 110(3-4):1005–1027, DOI 10.1007/s10584-011-0101-1

Swingedouw D, Terray L, Servonnat J, Guiot J (2012) Mechanisms for European summer temperature response to solar forcing over the last millennium. Climate of the Past 8(5):1487–1495, DOI 10.5194/cp-8-1487-2012

Telesca L, Lovallo M (2012) Analysis of seismic sequences by using the method of visibility graph. EPL (Europhysics Letters) 97(5):50,002

Telesca L, Lovallo M, Pierini JO (2012) Visibility graph approach to the analysis of ocean tidal records. Chaos, Solitons & Fractals 45(9):1086–1091

Telesca L, Lovallo M, Ramirez-Rojas A, Flores-Marquez L (2013) Investigating the time dynamics of seismicity by using the visibility graph approach: Application to seismicity of mexican subduction zone. Physica A 392(24):6571–6577

Telesca L, Lovallo M, Ramirez-Rojas A, Flores-Marquez L (2014) Relationship between the frequency magnitude distribution and the visibility graph in the synthetic seismicity generated by a simple stick-slip system with asperities. PloS One 9(8):e106,233, DOI 10.1371/journal.pone.0106233

Theiler J, Eubank S, Longtin A, Galdrikian B, Farmer JD (1992) Testing for nonlinearity in time series: the method of surrogate data. Physica D 58:77 – 94, DOI 10.1016/0167-2789(92)90102-S

Trouet V, Esper J, Graham NE, Baker A, Scourse JD, Frank DC (2009) Persistent positive North Atlantic oscillation mode dominated the Medieval Climate Anomaly. Science 324(5923):78–80, DOI 10.1126/science.1166349

Trouet V, Scourse J, Raible C (2011) North Atlantic storminess and Atlantic Meridional Overturning Circulation during the last Millennium: Reconciling contradictory proxy records of NAO variability. Global and Planetary Change 84:48–55, DOI 10.1016/j.gloplacha.2011.10.003

Yu Z, Anh V, Eastes R, Wang DL (2012) Multifractal analysis of solar flare indices and their horizontal visibility graphs. Nonlinear Processes in Geophysics 19(6):657–665

Zanchettin D, Timmreck C, Graf HF, Rubino A, Lorenz S, Lohmann K, Krüger K, Jungclaus JH (2011) Bi-decadal variability excited in the coupled oceanatmosphere system by strong tropical volcanic eruptions. Climate Dynamics 39(1-2):419–444, DOI 10.1007/s00382-011-1167-1

Zhong Y, Miller GH, Otto-Bliesner BL, Holland MM, Bailey DA, Schneider DP, Geirsdottir A, Dyn C (2011) Centennial-scale climate change from decadally-paced explosive volcanism: a coupled sea ice-ocean mechanism. Climate Dynamics 37(11-12):2373–2387, DOI 10.1007/s00382-010-0967-z

Zorita E, von Storch H, Gonzalez-Rouco FJ, Cubasch U, Luterbacher J, Legutke S, Fischer-Bruns I, Schlese U (2004) Climate evolution in the last five centuries simulated by an atmosphere-ocean model: global temperatures, the North Atlantic Oscillation and the Late Maunder Minimum. Meteorologische Zeitschrift 13(4):271–289, DOI 10.1127/0941-2948/2004/0013-0271

Zou Y, Donner R, Marwan N, Small M, Kurths J (2014a) Long-term changes in the north–south asymmetry of solar activity: a nonlinear dynamics characterization using visibility graphs. Nonlinear Processes in Geophysics, 21: 1113–1126, DOI 10.5194/npg-21-1113-2014

Zou Y, Small M, Liu Z, Kurths J (2014b) Complex network approach to characterize the statistical features of the sunspot series. New Journal of Physics 16(1):013051